I. Systems Analysis Research

SYSTEMS DIVISION

A. Recent Development Ephemerides and the Mass of Mercury, W. G. Melbourne and

D. A. O'Handley

The ephemeris development activity has completed the revision of the radar data set to reflect the current available information. A new determination of the mass of Mercury has been made.

Developmental ephemeris (DE) 40[1] was the last DE fit to planetary radar and optical data. A version of DE 40 (DE 43[2]) has an updated lunar ephemeris (LE) 6 (Ref. 1) instead of LE 4, which is on the DE 40 tapes.

Since the announcement of DE 40 on March 29, 1968, the radar data set has been expanded (Table 1).

Eighty-six observations from Arecibo, taken in 1967, have been removed from the current data set because of their anomalous character with respect to other observations made during the same time interval. An additional four Venus observations were removed because they had residuals of over 3σ when compared with DE 40.

Having completed this updating of the data set, a series of ephemerides were made. Initially, the data set was compared with DE 40 and a solution made for 21 parameters (SPS 37-51, Vol. III, pp. 4–13). Most of the corrections, although small, were significant to at least one figure with respect to the formal standard deviations (Table 2).

As seen in Table 2, the astronomical unit (AU) and radii of Venus and Mars were not changed significantly from the DE 40 values. The correction to the radius of

Table 1. Radar-range data status

Planet	Observatory	Number	Period
Mercury[a]	Arecibo	157	1964–1968
	Haystack	63	1967
Venus[b]	Arecibo	106	1964, 1965/1966, 1968
	JPL	284	1964–1967
	Haystack	49	1967
	Millstone	101	1964–1967
Mars	Arecibo	39	1964/1965
	Haystack	10	1967
[a]This data set includes the following additions:			
Mercury	Arecibo	11	14 May, 1968–9 June, 1968
	Haystack	63	26 Oct, 1966–12 Sept, 1967
[b]This data set includes the following additions:			
Venus	Arecibo	4	10 May, 1968–21 May, 1968

Note: The additional Mercury and Venus Arecibo, and Mercury Haystack, observations were provided by I. I. Shapiro in private communications to the authors.

Table 2. Planetary radius and astronomical unit values

Radius unit	DE 40 value, km	Correction to DE 40 value, km
Planetary radius		
Mercury	2437.3	$+8.7 \pm 0.5$
Venus	6055.8	$+0.7 \pm 0.4$
Mars	3375.3	$+0.3 \pm 12.4$
Astronomical unit		
—	149, 597, 895.8	$+1.3 \pm 0.4$

[1]O'Handley, D. A., *Announcement of JPL Developmental Ephemerides 39 and 40,* Mar. 29, 1968 (JPL internal documents).

[2]Mulholland, J. D., *Announcement of Developmental Ephemeris 43,* July 24, 1968 (JPL internal document).

Mercury was significant and reflects the expansion of the data set.

The DE 45 was created by applying these corrections to the DE 40 starting conditions at epoch JD 244 0800.5. The time span is JD 243 8400.5 to 244 0800.5 (January 6, 1964 to August 2, 1970). The planetary masses used in this integration were those given in SPS 37-45, Vol. IV, pp. 17–19. A comparison of DE 45 with the radar observations and a subsequent solution indicated that no further iteration was required for this set of data.

As reported in SPS 37-51, Vol. III, a definite signature appeared in the residuals of Venus time-delay measurements taken during 1965–1966 (see p. 10, Fig. 7, of SPS 37-51, Vol. III). At that time, it was conjectured that this effect might be due to second-order effects of fixed parameters. Also, intensive studies were made in search of program errors in the solar-system data processing system (SSDPS), and the choice of planetary masses came under scrutiny. Although Venus, earth–moon, and Mars mass values are very precisely known due to spacecraft radio tracking, the mass of Mercury has been poorly determined since its value depends on perturbation analyses of neighboring and minor planets. Clemence (Ref. 2) discusses the various determinations of the mass of Mercury and, in terms of reciprocal solar masses, the variation of the individual determinations amount to 8% of the quoted value. Subsequently, a brief analysis of "periodic perturbations of the longitude and radius vector of Venus" from Newcomb's Tables verified that a variation of this size in the mass of Mercury produced an effect on Venus time-delay observables of the same order of magnitude as the observed signature. This suggests the possibility of improving the mass of Mercury with radar observations.

Since the SSDPS does not presently generate partial derivatives of observables with respect to the mass of a perturbing body, the direct method of searching for the minimum of the weighted sum of the squared residuals was followed. Toward this end, several DEs spanning the 1964–1968 radar observation period were generated by setting the mass of Mercury to different values covering the neighborhood of uncertainty. The masses of the other planets were fixed at the values given in Ref. 3. The initial conditions in each of these ephemerides are identical with those of DE 45. In each case, a weighted least-squares fit of the up-dated radar data set discussed above, using the 21-parameter model, was performed to provide parameter corrections and predicted residuals for the subsequent iteration. However, subsequent iteration was unnecessary

because the corrections were small enough that non-linear effects could be neglected. Table 3 identifies the developmental ephemeris, the reciprocal mass of Mercury, $M_{\breve{\varphi}}^{-1}$, and the weighted sum-of-squares of the residuals after the fit, Σv^2. Here, Σv^2 is given by

$$\Sigma v^2 = \sum_{i=1}^{N} \left(\frac{O_i - C_i}{\sigma_i} \right)^2$$

where O is the observation, C is the predicted observation, and σ is the assigned standard deviation of the measurement.

Figure 1 exhibits the quadratic variation of Σv^2 with $M_{\breve{\varphi}}^{-1}$. The minimum corresponds to a value of $M_{\breve{\varphi}}^{-1} = 5.988 \times 10^6 \pm 10,000$. The formal standard devi-

Table 3. DEs spanning the 1964–1968 radar observation period

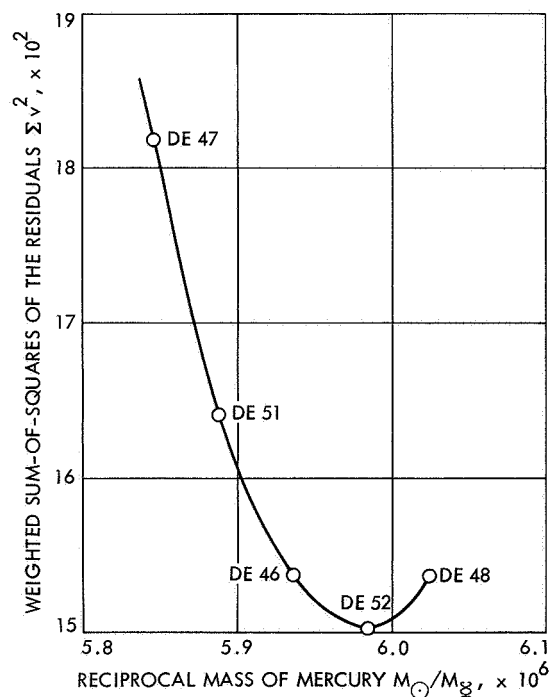| DE	$M_{\breve{\varphi}}^{-1} \times 10^{-6}$	Σv^2
47	5.845	1818.22
51	5.890	1641.02
46	5.935	1537.42
48	6.025	1538.17
52	5.984	1504.52

Fig. 1. The quadratic variation of Σv^2 with $M_{\breve{\varphi}}^{-1}$

ation of 10,000 quoted here is obtained from the curvature of the quadratic at the minimum point. It may be shown from estimation theory that

$$\sigma_{M_{\varphi}^{-1}} = \left[\frac{1}{2} \frac{d^2 \sum v^2}{d(M_{\varphi}^{-1})^2} \right]^{-\frac{1}{2}}$$

evaluated at the minimum point corresponds to the standard deviation of the estimated parameter obtained from

the covariance matrix for the case where M_{φ}^{-1} is included as one of the simultaneously estimated least-squares parameters. It should be stressed that this is a formal error and that this result is predicated on fixed mass values of the other planets.

It is possible to determine mass values of all of the inner planets in a simultaneous solution using the radar and optical observations of the planets. This has been
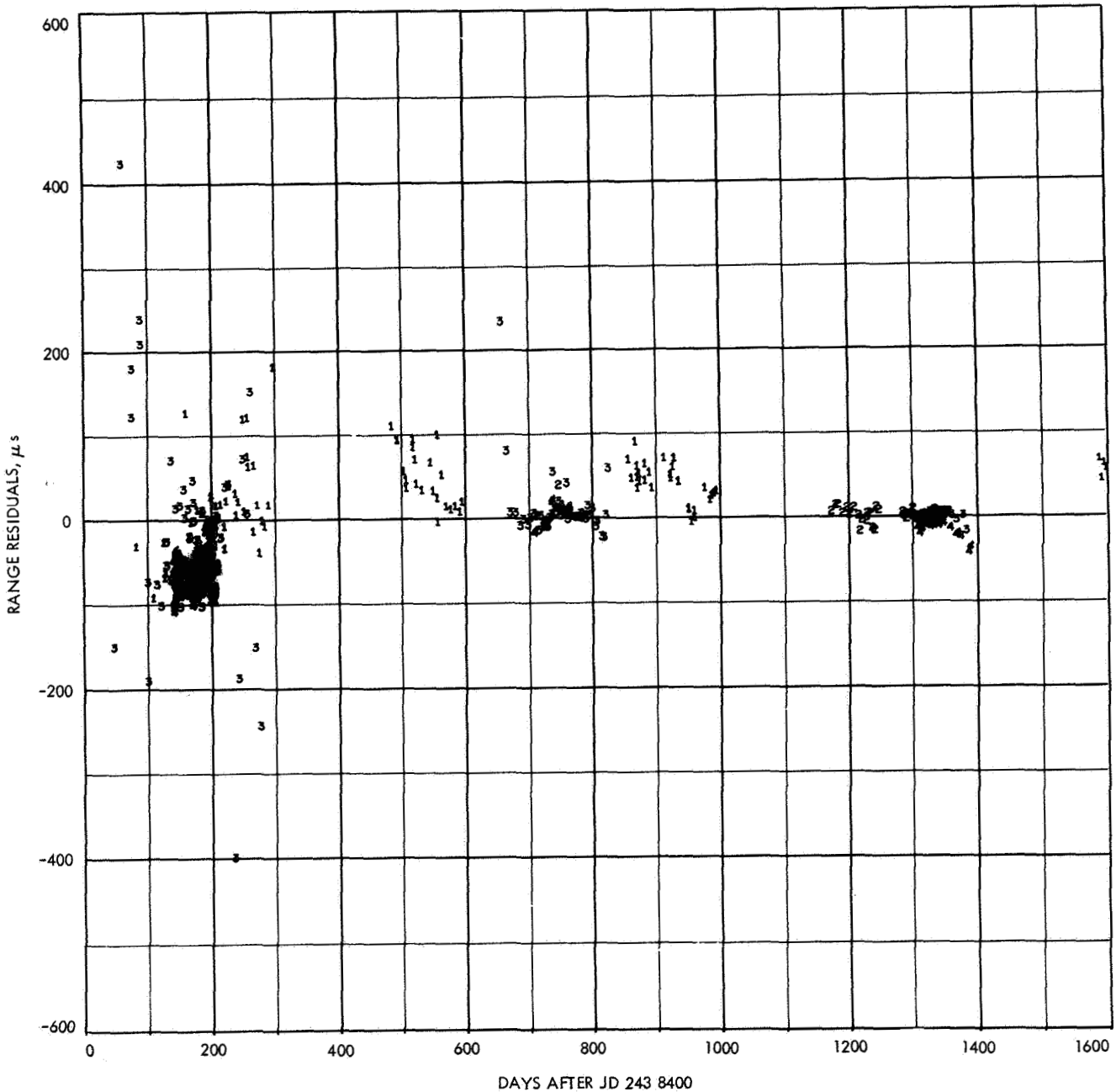

Fig. 2. Venus range residuals after fit to DE 52

done at MIT and the values of the reciprocal masses and the formal probable errors are as follows:[a]

Mercury	5,935,000 ± 45,000
Venus	408,536.5 ± 95
Earth–moon	328,896 ± 57
Mars	3,116,350 ± 6,400

The mass ratio of the earth–moon is 81.301 ±0.002. While these MIT mass values for Venus, earth–moon, and Mars are consistent with the values obtained for these quantities from the *Ranger* and *Mariner* series of spacecraft, the latter estimates are about two orders of magnitude more precise. For this reason, it has been decided to fix the mass values of these planets at their spacecraft-determined values until it becomes practicable to simultaneously process radio tracking and radar data.

Figure 2 shows the Venus range residuals after the fit to DE 52; the anomaly around the January 1966 inferior conjunction has nearly disappeared. The conclusion to be drawn from this work is that the feature in the radar-range residuals must be regarded as an anomaly in the modeling of the masses. If one considers the masses better known from spacecraft tracking, and therefore sets the values as known, the reduction of degrees of freedom will cause the "feature" to appear in the Venus residuals. By altering the mass of Mercury, the feature does disappear and the over-all sum of squared residuals is diminished.

References

1. Mulholland, J. D., *JPL Lunar Ephemeris Number 6*, Technical Memorandum 33-408. Jet Propulsion Laboratory, Pasadena, Calif., Oct. 15, 1968.

2. Clemence, G. M., "Masses of the Principal Planets." Joint Discussion on the Report of the Working Group on the IAU System of Astronomical Constants. *Trans. IAU*, Vol. XII B, p. 610, 1966.

3. Melbourne, W. G., et al., *Constants and Related Information for Astrodynamic Calculations, 1968*, Technical Report 32-1306. Jet Propulsion Laboratory, Pasadena, Calif., July 15, 1968.

B. A New Variation-of-Parameters Method With Universal Variables, R. Broucke

The classical variation-of-parameters methods, with the classical osculating orbit elements, have the disadvantage of not being uniformly valid for all types of conic orbits and all eccentricities or inclinations. This is essentially

[a] Private correspondence from I. I. Shapiro.

due to the particular representation of the conic orbit that is used. It is well known that solutions of the two-body problem exist that include, in one single formulation, the elliptic, parabolic, hyperbolic, and rectilinear cases. In these formulations, no particular attention has to be given to the small eccentricity or small inclination situations. In the recent past, several perturbation techniques have been produced that take advantage of the universal formulation of the two-body problem; e.g., S. Herrick (Ref. 1), R. H. Battin (Ref. 2), S. Pines (Ref. 3), W. H. Goodyear (Refs. 4 and 5), and others.

In the present article, a new method of variation of parameters (variation of arbitrary constants) with universal variables is given that seems to be more simple in form than most of the existing methods. It is generally accepted that a method of variation of parameters uses osculating orbits, and that the Encke method of computing perturbations uses a fixed Keplerian reference orbit. The remarkable feature of the new method described in this article is that it uses a fixed Keplerian reference orbit, but no osculating orbits or osculating orbit elements.

In previous works on variation-of-parameters methods with universal variables, six first-order differential equations for the initial positions, x_0, and velocity, v_0, of the osculating Keplerian orbits are always obtained. In the work discussed herein, six similar first-order differential equations are also obtained, but a fixed Keplerian reference orbit is used. This reference orbit could be osculating either at some instant or at the epoch, or it could be some well-chosen mean orbit, but this is by no means essential.

In terms of the x_0 and v_0 vectors, the equation for the two-body reference orbit may be written as

$$\left. \begin{array}{l} x_R = f x_0 + g v_0 \\ \dot{x}_R = \dot{f} x_0 + \dot{g} v_0 \end{array} \right\} \tag{1}$$

For an elliptic orbit, the functions f, g and their derivatives are

$$\left. \begin{array}{l} f = \dfrac{a}{r_0}(\cos\theta - 1) + 1 \\[2mm] g = t - \dfrac{1}{n}(\theta - \sin\theta) \\[2mm] \dot{f} = -\dfrac{a^2 n}{r_R r_0}\sin\theta \\[2mm] \dot{g} = 1 + \dfrac{a}{r_R}(\cos\theta - 1) \end{array} \right\} \tag{2}$$

where $\theta = E - E_0$ is the difference between the eccentric anomalies at time $t(E)$ and time $t = 0 (E_0)$. In general, the subscript 0 refers here to the values at the time $t = 0$.

The different elements used in Expression (2) refer to the reference orbit rather than the true perturbed orbit. The functions f and g have several interesting properties; for instance, the Wronskian determinant of f and g is

$$f\dot{g} - \dot{f}g = +1 \qquad (3)$$

In fact, Eq. (3) is equivalent to Kepler's equation. On the other hand, the f and g functions are solutions of the fundamental two-body differential equations

$$\left. \begin{array}{c} \ddot{f} = -\mu \dfrac{f}{r_R^3} \\[2mm] \ddot{g} = -\mu \dfrac{g}{r_R^3} \end{array} \right\} \qquad (4)$$

Expression (1) is valid for all types of conics at the condition to choose the right f and g functions. A universal formulation has been produced by R. H. Battin (Ref. 2, p. 52, Eqs. 2.43 and 2.44) wherein he gives f and g functions containing two special transcendental functions S and C that generalize $\sin \theta$ and $\cos \theta$ in Expression (2). Also, S. Herrick has given several different forms of f and g functions in his study on the use of universal variables in the two-body problem (Ref. 1). The following derivation of a variation-of-parameters method is valid if either Battin's or anyone of the sets of f and g functions given by Herrick are used.

Let us first derive the variational equations. The equations of motion for the unperturbed reference motion are

$$\ddot{\mathbf{x}}_R = -\mu \frac{\mathbf{x}_R}{r_R} \qquad (5)$$

and the corresponding equations for the perturbed motion are

$$\ddot{\mathbf{x}} = -\mu \frac{\mathbf{x}}{r^3} + \mathbf{X} \qquad (6)$$

where $\mathbf{X}$ is the perturbing acceleration vector. Now defining the perturbations by

$$\delta\mathbf{x} = \mathbf{s} = \mathbf{x} - \mathbf{x}_R \qquad (7)$$

we obtain, by subtracting Eq. (5) from Eq. (6), the following second-order differential equations for the com-

ponents of $\mathbf{s}$:

$$\mathbf{s} + \mu \frac{\mathbf{s}}{r_R^3} = -\mu \left(\frac{1}{r^3} - \frac{1}{r_R^3} \right) \mathbf{x} + \mathbf{X} = \mathbf{F} \qquad (8)$$

Thus, this is a system of non-linear differential equations called the variational equations or the "perturbation equations." Since Expression (8) is exact and is not limited to the first order, it should not be confused with the well-known first-order variational equations because no approximation and no expansion has been made in deriving it. By comparison with Expression (4), we see that the homogeneous differential equations corresponding to Expression (8) have the general solution

$$\mathbf{s} = \mathbf{K}_1 f + \mathbf{K}_2 g \qquad (9)$$

where $\mathbf{K}_1$ and $\mathbf{K}_2$ are the six arbitrary constants. We will transform Eq. (9) in such a way that by replacing the constants $\mathbf{K}_1$ and $\mathbf{K}_2$ with the appropriate functions of time, the same expression for $\mathbf{s}$ is a solution of the non-homogeneous equations. This is accomplished using the standard method of solving non-homogeneous linear differential equations with Lagrange's method of variation of arbitrary constants. We may *a priori* give the relation between the components of $\mathbf{K}_1$ and $\mathbf{K}_2$ as

$$\dot{\mathbf{K}}_1 f + \dot{\mathbf{K}}_2 g = 0 \qquad (10)$$

so that the derivative of $\mathbf{s}$ in Eq. (9) is

$$\dot{\mathbf{s}} = \mathbf{K}_1 \dot{f} + \mathbf{K}_2 \dot{g} \qquad (11)$$

Taking the second derivative of $\mathbf{s}$, and using the relations given in Expression (4), we obtain the equation

$$\dot{\mathbf{K}}_1 \dot{f} + \dot{\mathbf{K}}_2 \dot{g} = \mathbf{F} \qquad (12)$$

Combining Eqs. (10) and (12) now gives a system of six ordinary equations in the first derivatives of the six components of the vectors $\mathbf{K}_1$ and $\mathbf{K}_2$:

$$\left. \begin{array}{c} \dot{\mathbf{K}}_1 f + \dot{\mathbf{K}}_2 g = 0 \\[2mm] \dot{\mathbf{K}}_1 \dot{f} + \dot{\mathbf{K}}_2 \dot{g} = \mathbf{F} \end{array} \right\} \qquad (13)$$

Using the property given in Eq. (3), we can write the solution of Expression (13) in the form

$$\left. \begin{array}{c} \dot{\mathbf{K}}_1 = -g\,\mathbf{F} \\[2mm] \dot{\mathbf{K}}_2 = +f\,\mathbf{F} \end{array} \right\} \qquad (14)$$

and this is the desired final result. In Expression (14), there are six first-order differential equations that can be used for solution by numerical integration as a variation-of-parameters method, or also for the generation of a solution in the form of an iterative general perturbation theory.

The result given in Expression (14) may be written in a slightly different form:

$$x = x_R + s = (x_0 + K_1)f + (v_0 + K_2)g \qquad (15)$$

Now we introduce two new vectors

$$\left. \begin{array}{l} X_0 = x_0 + K_1 \\ V_0 = v_0 + K_2 \end{array} \right\} \qquad (16)$$

which differ from K_1 and K_2 only by the addition of a constant vector so that for X_0, V_0, we have the same differential equations as in Expression (14):

$$\left. \begin{array}{l} \dot{X}_0 = -g\,F \\ \dot{V}_0 = +f\,F \end{array} \right\} \qquad (17)$$

The coordinates in the perturbed orbit are thus given by

$$x = X_0 f + V_0 g \qquad (18)$$

As a consequence of Eq. (10), the velocity components are given by

$$\dot{x} = X_0 \dot{f} + V_0 \dot{g} \qquad (19)$$

i.e., Eq. (18) has to be differentiated as if X_0 and V_0 were constants, although they are functions of time, to be obtained by the integration of the first-order differential Expression (17). It is remarkable that the expressions for the coordinates and velocity in the perturbed orbit, as given by Eqs. (18) and (19), are so similar to the corresponding Expression (1) in a Keplerian orbit.

References

1. Herrick, S., "Universal Variables," *Astron. J.*, Vol. 70, No. 4, pp. 309–315, May 1965.

2. Battin, R. H., *Astronautical Guidance*, McGraw-Hill Book Co., Inc., New York, 1964.

3. Pines, S., "Variation of Parameters for Elliptic and Near Circular Orbits," *Astron. J.*, Vol. 66, No. 1, pp. 5–7, Feb. 1961.

4. Goodyear, W. H., "Completely General Closed-Form Solution for Coordinates and Partial Derivatives of the Two-Body Problem," *Astron. J.*, Vol. 70, No. 3, pp. 189–192, April 1965.

5. Goodyear, W. H., "A General Method of Variation of Parameters for Numerical Integration," *Astron. J.*, Vol. 70, No. 8, pp. 524–526, Oct. 1965.

C. Optimization of a Solar Electric Propulsion Planetary Orbiter Spacecraft, C. G. Sauer, Jr.

1. Introduction

For the past several years there has been a great deal of interest in combining large solar-array power systems with electric-propulsion thrusters for unmanned exploration of the solar system. In particular, a Jupiter flyby mission has been studied quite extensively (Refs. 1–5). In order to determine the feasibility of a solar electric propulsion (SEP) spacecraft for a particular mission, the increase in performance must be balanced against the greater cost and increased complexity, and hence possibly lower reliability, of the SEP spacecraft as compared with that of an equivalent ballistic spacecraft.

Since the SEP spacecraft being considered in the various studies have a relatively low specific power, the thrust acceleration is also quite low (10^{-5} to 5×10^{-5} g), and the use of low-thrust spiral trajectories for the escape and capture phases of the mission is precluded because of the extremely long flight times that would result. Thus, the missions being analyzed use the launch vehicle to provide some fraction of the energy required for the mission over that energy required for the initial earth parking orbit. Also, for an orbiter mission, a relatively high-thrust chemical retro-propulsion maneuver is used to place the spacecraft into the specified planetary orbit. It is, consequently, impossible to make a clear distinction between the launch vehicle and the SEP spacecraft in the mission analysis, and an optimization cannot be performed that separates the heliocentric and planet-centered phases of the mission.

2. Trajectory Optimization

The kinematic aspects of the trajectory optimization are only briefly considered here since a thorough analysis has been made by a number of previous investigators (Refs. 3 and 6). A two-body optimization of the trajectory of a thrusting SEP low-thrust spacecraft is made that simultaneously solves the equations of motion and the variational equations. The program used in this analysis has the capability of optimizing not only the path of the spacecraft, but also certain vehicle parameters such as thruster specific impulse or solar-panel output power. In addition, the program allows for coast phases of flight during the mission.

To account for the effects of the departure and arrival planets on the performance estimates to be obtained, an asymptotic velocity bias method is employed (SPS 37-36, Vol. IV, pp. 14–19, and Ref. 7). This method is based upon the observation that for the case of a thrusting spacecraft in the gravitational field of a planet, the planet-centered velocity of the spacecraft approaches an asymptotic form as the spacecraft recedes from the planet and the gravitational effects of the planet become negligible. The extrapolation of this asymptotic form to "zero" time serves to define an initial velocity bias such that a thrusting spacecraft departing from a massless planet with this initial velocity would have this asymptotic form as its velocity profile. This asymptotic velocity bias is then used to bias the initial velocity or final velocity as specified by the ephemeris of the departure or arrival planets.

The differential equations serving to define the velocity V and position R of the spacecraft are given by

$$\dot{\mathbf{V}} = -\nabla U + a\zeta \tag{1}$$

$$\dot{\mathbf{R}} = \mathbf{V} \tag{2}$$

where the gravitational potential U is given by

$$U = -\frac{GM}{r} \tag{3}$$

for an inverse-square central force field. The magnitude of the vector position R is given by r. The magnitude a of the thrust acceleration in Eq. (1) is given by

$$a = 2\frac{P_T}{mc} \tag{4}$$

where P_T is the thruster output power, m is the vehicle mass, and c is the effective exhaust velocity of the thrusters. The thrust is aligned in a direction given by the unit thrust vector ζ. The mass of the spacecraft is found by solving the differential equation

$$\dot{m} = -2\frac{P_T}{c^2} \tag{5}$$

The P_T is equal to the thruster electrical input power P_I decreased by the efficiency factor η of the thrusters:

$$P_T = \eta P_I \tag{6}$$

This thruster efficiency is a function of the power conditioning efficiency, thruster mass utilization, and other losses in the thrusters proportional to the thruster specific impulse.

When a requirement exists for an additional power drain from the solar panels for a spacecraft auxiliary power requirement, the P_I is not equal to the solar-panel output power P, but rather to this power decreased by the auxiliary power requirement ΔP:

$$P_I = P - \Delta P \tag{7}$$

Since P and P_I are not necessarily equal, an overall powerplant specific mass, which includes both solar-panel and thruster specific masses, must be defined and used with caution. When an auxiliary power requirement exists, the overall specific mass must be separated into a solar-panel specific mass α_w defined by

$$\alpha_w = \frac{m_w}{P_0} \tag{8}$$

and a thruster subsystem specific mass α_{th} defined by

$$\alpha_{th} = \frac{m_{th}}{P_I} = \frac{m_{th}}{P_0 - \Delta P} \tag{9}$$

The P_0 at 1 AU is used to define α_w.

The overall powerplant mass m_{pp}, defined as the sum of the solar-panel mass m_w, and the thruster mass m_{th} is given by

$$m_{pp} = m_w + m_{th} = (\alpha_w + \alpha_{th})P_0 - \alpha_{th}\Delta P \tag{10}$$

or

$$m_{pp} = \alpha P_0 - \alpha_{th}\Delta P \tag{11}$$

with the overall specific mass α being given by

$$\alpha = \alpha_w + \alpha_{th} \tag{12}$$

A constant power drain from the solar panels complicates the analysis since the panel output power varies as a function of the distance of the spacecraft from the sun. Denoting $\gamma_p(r)$ as the normalized variation of P with solar distance r, P is given by

$$P = P_0 \gamma_p(r) \tag{13}$$

and the P_I is consequently

$$P_I = P_0 \gamma_p(r) - \Delta P \tag{14}$$

The thrust acceleration [Eq. (4)] and mass [Eq. (5)] can thus be given as a function of P_0:

$$a = \frac{2\eta}{mc}\left[P_0\,\gamma_p\,(r) - \Delta P\right] \qquad (15)$$

$$\dot{m} = -\frac{2\eta}{c^2}\left[P_0\,\gamma_p\,(r) - \Delta P\right] \qquad (16)$$

Two additional differential equations are considered in the formulation, although they are not actually used in the trajectory program. These equations

$$\dot{P}_0 = 0 \qquad (17)$$

and

$$\dot{c} = 0 \qquad (18)$$

serve to define two vehicle parameters that can be optimized.

The modified Hamiltonian H for this problem is

$$H = -\left(\boldsymbol{\lambda}\cdot\mathbf{V} + \dot{\boldsymbol{\lambda}}\cdot\nabla U\right) + \frac{2\eta}{m_0 c}\left[P_0\gamma_p\,(r) - \Delta P\right]L \qquad (19)$$

where m_0 denotes the initial mass of the spacecraft and L is the so-called thrust switching function (Ref. 6) defined by

$$L = \frac{\boldsymbol{\zeta}\cdot\boldsymbol{\lambda}}{m/m_0} - \frac{m_0}{c}\lambda_m \qquad (20)$$

and determines the periods of propulsion and coasting from

$$P_T = P_0\gamma_p\,(r) - \Delta P\,, \qquad L > 0 \qquad (21)$$

$$P_T = 0\,, \qquad L < 0 \qquad (22)$$

In Eq. (19), the $\boldsymbol{\lambda}$ are a set of LaGrange multipliers conjugate to the position and velocity of the spacecraft, and λ_m is the multiplier conjugate to the mass of the spacecraft. The Euler–LaGrange equations resulting from Eq. (19) are

$$\ddot{\boldsymbol{\lambda}} = -\left(\boldsymbol{\lambda}\cdot\nabla\right)\nabla U + \frac{2\eta}{m_0 c}\left[P_0\,\nabla\gamma_p\,(r)\right]L \qquad (23)$$

for position and velocity and

$$\dot{\lambda}_m = \frac{2\eta}{m_0 c}\left[P_0\gamma_p\,(r) - \Delta P\right]\frac{\boldsymbol{\zeta}\cdot\boldsymbol{\lambda}}{m/m_0}\frac{1}{m} \qquad (24)$$

for spacecraft mass. During a coast period, the term containing $\nabla\gamma_p\,(r)$ in Eq. (23), and also the right-hand side of Eq. (24), are zero.

It is, perhaps, more convenient in the formulation to determine the thrust switching function from the differential equation

$$\dot{L} = \frac{\boldsymbol{\zeta}\cdot\dot{\boldsymbol{\lambda}}}{m/m_0} \qquad (25)$$

and then determine λ_m from

$$\lambda_m = \frac{c}{m_0}\left(\frac{\boldsymbol{\zeta}\cdot\boldsymbol{\lambda}}{m/m_0} - L\right) \qquad (26)$$

The calculus of variations also yields the condition that the unit thrust vector is aligned in the direction specified by the multiplier vector $\boldsymbol{\lambda}$:

$$\boldsymbol{\zeta} = \frac{\boldsymbol{\lambda}}{\lambda} \qquad (27)$$

where λ is the magnitude of the multiplier vector $\boldsymbol{\lambda}$. In addition, the multipliers conjugate to the power P_0 and to the thruster exhaust velocity c are given by the differential equations

$$\dot{\lambda}_P = -\frac{2\eta}{m_0 c}\gamma_p\,(r)\,L \qquad (28)$$

$$\dot{\lambda}_c = \frac{2\eta}{m_0 c^2}\left[P_0\gamma_p\,(r) - \Delta P\right]\left[\left(2 - c\frac{\eta'}{\eta}\right)L - \frac{\boldsymbol{\zeta}\cdot\boldsymbol{\lambda}}{m/m_0}\right] \qquad (29)$$

where η' is the derivative of η with respect to c.

The transversality condition that must be satisfied for this problem is given by

$$\left[-H\,dt + \boldsymbol{\lambda}\cdot d\mathbf{V} + \dot{\boldsymbol{\lambda}}\cdot d\mathbf{R} + \lambda_m\,dm + \lambda_P\,dP_0 + \lambda_c\,dc\right]_0^T = 0 \qquad (30)$$

The conditions required for optimizing P, c, and departure and arrival energy are derived from the transversality condition given in Eq. (30).

In the discussion that follows, we will consider the initial and final time specified so that $dt = 0$ at both endpoints of the trajectory. In addition we will assume an ephemeris is employed so that $d\mathbf{R} = 0$ at both endpoints

and that $d\mathbf{V}$ is given by

$$d\mathbf{V} = V_B \, d\xi + dV_B \xi \qquad (31)$$

where V_B is both the magnitude of the velocity bias and

a function of the departure or arrival energy, thrust acceleration, and gravitational attraction of the attracting planet. The unit vector ξ defines the direction in which the velocity bias is directed. The transversality condition given in Eq. (30) can thus be rewritten as

$$V_{BA} \lambda \cdot d\xi + dV_{BA} \lambda \cdot \xi - V_{BD} \lambda^0 \cdot d\xi - dV_{BD} \lambda^0 \cdot \xi + \lambda_m \, dm - \lambda_m^0 \, dm_0 + (\lambda_P - \lambda_P^0) \, dP_0 + (\lambda_c - \lambda_c^0) \, dc = 0 \qquad (32)$$

where subscripts A and D refer to values of V_B at arrival and departure, respectively, and superscript zeros denote the initial values of the multipliers. In order to optimize the direction in which the velocity bias is applied, the term $\lambda \cdot d\xi$ in Eq. (32) must be zero, implying that the velocity bias is aligned in, or opposed to, the direction defined by the multiplier vector λ. In addition, we can set

$$\lambda_c^0 = 0 \qquad (33a)$$

$$\lambda_P^0 = 0 \qquad (33b)$$

without any loss of generality.

In terms of the variables appearing in Eq. (32), dV_B can be expanded to

$$dV_B = \frac{\partial V_B}{\partial C_3} \, dC_3 + \frac{\partial V_B}{\partial a} \, da \qquad (34)$$

where C_3 is the vis viva energy. Since the thrust acceleration is a function of the m, c, and P, Eq. (34) becomes

$$dV_B = \frac{\partial V_B}{\partial C_3} \, dC_3 + \frac{\partial V_B}{\partial a} \frac{\partial a}{\partial c} \, dc + \frac{\partial V_B}{\partial a} \frac{\partial a}{\partial m} \, dm + \frac{\partial V_B}{\partial a} \frac{\partial a}{\partial P_0} \, dP_0 \qquad (35)$$

where dV_B is to be evaluated at each endpoint.

The transversality condition given in Eq. (32) can also be expanded into

$$-\lambda \frac{\partial V_{BA}}{\partial C_{3A}} \, dC_{3A} - \lambda^0 \frac{\partial V_{BD}}{\partial C_{3D}} \, dC_{3D} + \left\{ \lambda_m - \lambda \frac{\partial V_{BA}}{\partial a} \frac{\partial a}{\partial m} \right\} dm - \left\{ \lambda_m^0 + \lambda^0 \frac{\partial V_{BD}}{\partial a} \frac{\partial a}{\partial m_0} \right\} dm_0$$

$$+ \left\{ \lambda_P - \lambda \frac{\partial V_{BA}}{\partial a} \frac{\partial a}{\partial P_0} - \lambda^0 \frac{\partial V_{BD}}{\partial a} \frac{\partial a}{\partial P_0} \right\} dP_0 + \left\{ \lambda_c - \lambda \frac{\partial V_{BA}}{\partial a} \frac{\partial a}{\partial c} - \lambda^0 \frac{\partial V_{BD}}{\partial a} \frac{\partial a}{\partial c} \right\} dc = 0 \qquad (36)$$

where λ is the magnitude of the multiplier λ at arrival and λ^0 is the magnitude at departure, and subscripts A and D denote values of V_B and C_3 at arrival and departure, respectively. The direction of the velocity bias is opposite to that of the multiplier λ at arrival; hence, the terms containing V_{BA} have a negative sign associated with them.

Since c does not appear in any of the differentials in Eq. (36) except the last, this last term in Eq. (36) is the expression that must equal zero for c to be optimum.

3. Spacecraft and Payload Optimization

The previous development has been devoted exclusively to the SEP spacecraft. The m_0 of the spacecraft is a function only of the initial vis viva energy C_{3D} through the injected weight capability of the launch vehicle. Thus, the variations in the initial mass of the spacecraft can be directly related to variations in the value of the departure energy:

$$dm_0 = \frac{dm_0}{dC_{3D}} \, dC_{3D} \qquad (37)$$

The m_0 can be expressed in the following form as a function of the launch-vehicle characteristics m_s, m_d, and I_{sp}:

$$m_0 = m_s \exp\left(-\frac{V_G - V_P}{g_0 I_{sp}}\right) - m_d \qquad (38)$$

where V_P is the local parabolic velocity and V_G is given by

$$V_G = (V_P^2 + C_{3D})^{1/2} \qquad (39)$$

In order to match the net injected payload capability of the launch vehicle with the above constants, the specific impulse I_{sp} appearing in Eq. (38) will not necessarily equal the I_{sp} of the last stage. The term m_d appearing in Eq. (38) represents the net inert mass of the last stage of the injection vehicle, including payload adapter, that is discarded. The value of $m_s - m_d$ represents the net injected weight capability at a C_3 equal to zero. From Eq. (38), the variation of m_0 can be expressed as

$$dm_0 = -\frac{m_0 + m_d}{2V_G g_0 I_{sp}} dC_{3D} \qquad (40)$$

There are two additional mass components of the low-thrust spacecraft that can be considered in the optimization. These are the structural mass m_{st} given by

$$m_{st} = k_{st} m \qquad (41)$$

where k_{st} is the structural factor of the spacecraft. The low-thrust propellant tankage mass m_{pt} is defined as

$$m_{pt} = k_{pt} m_p = k_{pt}(m_0 - m) \qquad (42)$$

where k_{pt} is the propellant tankage factor.

For the orbiter or rendezvous mission, there is an additional system to be defined—that of the retro-propulsion system. This system will be employed for the final capture maneuver at the target planet and consists of two parts: (1) the propellant mass, and (2) the retro-system inert mass including tankage and thruster. For the purposes of this analysis, the inert retro-system mass will be defined as a fixed fraction of the propellant mass m_{fl}:

$$m_r = k_r m_{fl} \qquad (43)$$

where k_r is the retro-system inert mass fraction.

At the point in the trajectory prior to the retro-maneuver, there are several options available. For example, we can jettison parts of the spacecraft for which there is no further use, such as the electric-propulsion engines or perhaps some fraction of the solar panels. We could also consider a re-entry package being discharged at this point. The particular spacecraft we will consider, however, is one in which the entire spacecraft less retro-propellant is orbited.

At the point where the retro-maneuver is made, the speed V_C of the spacecraft with respect to the target planet is given as a function of the vis viva energy C_{3A}:

$$V_C^2 = V_P^2 + C_{3A} \qquad (44)$$

where V_P is the local parabolic velocity at this point. Denoting the desired orbital speed after the capture maneuver by V_F, the velocity increment V_R due to the deboost maneuver is

$$V_R = V_C - V_F \qquad (45)$$

and the spacecraft mass m_g after the deboost maneuver is given by

$$m_g = m \exp\left(\frac{-V_R}{g_0 I_{sp}}\right) = m E \qquad (46)$$

The net payload m_f that we wish to maximize will be defined as the orbiting m_g less solar panels, electric-propulsion thrusters, structural mass, low-thrust propellant tankage mass, and retro-system inert mass:

$$m_f = m_g - m_w - m_{th} - m_{st} - m_{pt} - m_r \qquad (47)$$

Since the m_{fl} is given by

$$m_{fl} = m - m_g \qquad (48)$$

the m_f can be rewritten as, using Eqs. (41), (42), and (43),

$$m_f = [(1 + k_r) E - k_{st} + k_{pt} - k_r] m - m_w - m_{th} - k_{pt} m_0 \qquad (49)$$

The change in m_f due to changes in m, m_w, m_{th}, m_0, and C_{3A} is consequently given by

$$dm_f = [(1 + k_r) E - k_{st} + k_{pt} - k_r] dm - dm_w - dm_{th} - k_{pt} dm_0 + \left[(1 + k_r) m \frac{\partial E}{\partial C_{3A}}\right] dC_{3A} \qquad (50)$$

From Eqs. (8) and (9)

$$dm_w = \alpha_w \, dP_0 \qquad (51)$$

and

$$dm_{th} = \alpha_{th} \, dP_0 \qquad (52)$$

so that Eq. (50) can be rewritten as

$$dm = \frac{1}{(1 + k_r)\, E - k_{st} + k_{pt} - k_r} \left\{ dm_f + \alpha dP_0 + k_{pt}\, dm_0 - \left[(1 + k_r)\, m\, \frac{\partial E}{\partial C_{3A}} \right] dC_{3A} \right\} \qquad (53)$$

By substituting Eqs. (53) and (37) into Eq. (36)

$$\lambda_m^*\, dm_f = \left[\lambda_m^*\, (1 + k_r)\, m\, \frac{\partial E}{\partial C_{3A}} + \lambda\, \frac{\partial V_{BA}}{\partial C_{3A}} \right] dC_{3A} + \left[\lambda^0 \frac{\partial V_{BD}}{\partial C_{3D}} + \left(\lambda_m^0 + \lambda^0 \frac{\partial V_{BD}}{\partial m_0} - \lambda_m^* \, k_{pt} \right) \frac{dm_0}{dC_{3D}} \right] dC_{3D}$$

$$+ \left(-\lambda_P + \lambda\, \frac{\partial V_{BA}}{\partial P_0} + \lambda^0 \frac{\partial V_{BD}}{\partial P_0} - \lambda_m^* \, \alpha \right) dP_0 + \left(-\lambda_c + \lambda\, \frac{\partial V_{BA}}{\partial c} + \lambda^0 \frac{\partial V_{BD}}{\partial c} \right) dc \qquad (54)$$

where λ_m^* is given by

$$\lambda_m^* = \frac{\lambda_m - \lambda\, \dfrac{\partial V_{BA}}{\partial a}\, \dfrac{\partial a}{\partial m}}{(1 + k_r)\, E - k_{st} + k_{pt} - k_r} \qquad (55)$$

The functions in Eq. (54) are those to be used in maximizing m_f with respect to arrival C_3, departure C_3, P, and c.

By considering the definition of E in Eq. (46), we can set

$$\frac{\partial E}{\partial C_{3A}} = -\frac{E}{g_0 I_{sp}}\, \frac{1}{2 V_{CA}} \qquad (56)$$

in Eq. (54). The remaining terms appearing in Eqs. (54) and (55) still to be defined are those that are functions of the velocity bias at the departure or arrival planets.

Rather than using the expressions derived in SPS 37-36, Vol. IV and Ref. 7, an approximation is made that allows the partial derivatives to be more easily calculated and, furthermore, eliminates a discontinuity in the derivatives. The velocity bias is of the form

$$V_B = F(x)\, (GM\, a)^{1/4} \qquad (57)$$

where

$$x = \frac{C_3}{4\, (GM\, a)^{1/2}} \qquad (58)$$

and the function $F(x)$, which in the references quoted contains elliptic integrals, is of the form

$$F(x) = 2 \frac{(x + 0.651630)\, (x + 4.113609)\, (x + 1.214342)}{(x + 4.169068)\, (x + 1.303312)\, (x + 1)^{1/2}} \qquad (59)$$

Note that the above approximation is invalid for values of the parameter x that are less than or equal to -1; in fact, the approximation should not be used for values of x less than around -0.6 since the asymptotic velocity bias method that is used to calculate V_B starts to deteriorate in accuracy at about this point. The actual path of the spacecraft for escape at this value of x would appear more like a one-turn skewed spiral escape. An additional observation of the above approximation is that the velocity bias asymptotically approaches the hyperbolic excess velocity as the *vis viva* energy C_3 becomes large.

References

1. *Solar-Powered Electric Propulsion Summary Report*, Report SD-60374R, Hughes Aircraft Co., Culver City, Calif., Dec. 1966.
2. Stearns, J. W., and Kerrisk, D. J., "Solar-Powered Electric Propulsion Systems—Engineering and Applications," Paper 66-576, presented at the AIAA Second Propulsion Joint Specialist Conference, Colorado Springs, Colo., June 1966.
3. Dickerson, W. D., and Smith, D. B., "Trajectory Optimization for Solar-Electric Powered Vehicles," Paper 67-583, presented at the AIAA Guidance, Control and Flight Dynamics Conference, Huntsville, Ala., Aug. 1967.

4. Flandro, G. A., and Barber, T. A., "Mission Analysis for In-
   terplanetary Vehicles With Solar-Electric Propulsion," Paper
   67-708, presented at the AIAA Electric Propulsion and Plasma-
   dynamics Conference, Colorado Springs, Colo., Sept. 1967.

5. Sauer, C. G., Jr., "Trajectory Analysis and Optimization of a
   Low-Thrust Solar-Electric Jupiter Flyby Mission," Paper 67-710,
   presented at the AIAA Electric Propulsion and Plasmadynamics
   Conference, Colorado Springs, Colo., Sept. 1967.

6. Melbourne, W. G., and Sauer, C. G., "Optimum Thrust Pro-
   grams for Power-Limited Propulsion Systems," *Astronaut. Acta*,
   Vol. VIII, Fasc. 4, 1962.

7. Fimple, W. R., and Edelbaum, T. N., *Study of Low-Acceleration
   Space Transportation Systems*, Report D-910262-3, United Air-
   craft Corp., East Hartford, Conn., July 1965.

Fig. 3. Potential at P due to mascon at Q_i

D. Representation of Point Masses by Spherical Harmonics, *J. Lorell*

1. Introduction

The recent work by W. L. Sjogren and P. M. Muller
(Ref. 1) suggests that part of the lunar mass inhomo-
geneity consists of a few isolated mass concentrations
scattered across the lunar surface. Sjogren and Muller
have used *Lunar Orbiter* tracking data to identify several
of these high-density regions and named them "mascons."
By incorporating these mascons in the moon gravity
model, it is hoped that the *Lunar Orbiter* tracking data
fits can be much improved.

The basic computer programs presently used for *Lunar
Orbiter* orbit determination (OD) use a moon gravity
model expressed in spherical harmonics. Inclusion of the
mascons as point mass potentials would require some
modification of these programs and would result in a
hybrid gravity model. On the other hand, the mascons
can be represented by spherical harmonics expansions
and the resulting coefficients used directly in the OD
program.

In this article, we will write the equations for spherical
harmonic expansion of mascons and apply same to a pre-
liminary moon model obtained from Sjogren and Muller.

2. Spherical Harmonic Expansion of Potential Due to Point Mass

The potential due to a point mass is given by the ex-
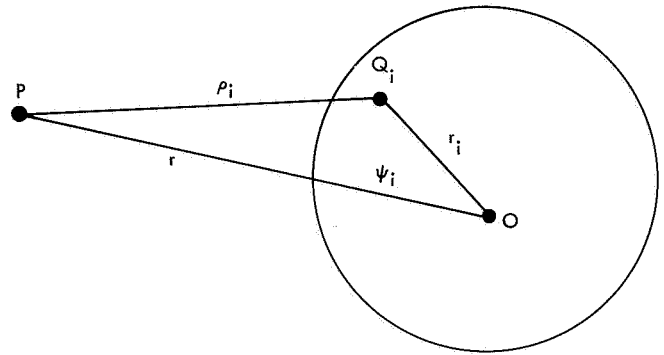pression $-\mu/\rho$, in which μ is the gravity constant giving

the size of the mass and ρ is the distance to the mass.
This potential is easily represented as a spherical har-
monic expansion centered at the point mass. What is
needed here, however, is the expansion about the center
of the moon, not the point mass that lies just below the
moon's surface. Let the mascon be located at a point
$Q_i (r_i, \theta_i, \lambda_i)$ located within the body of the moon whose
mass center is at 0 (see Fig. 3). Then the potential at
$P(r, \theta, \lambda)$ denoted by $\phi_i(r, \theta, \lambda)$ is given by

$$\phi_i = -\mu_i/\rho_i \tag{1}$$

where μ_i is the gravity constant of the mascon and ρ_i is
the distance from Q_i to P. Expanding in spherical har-
monics about Q_i gives

$$\phi_i = -\frac{\mu_i}{(r^2 + r_i^2 - 2r\,r_i \cos\psi_i)^{1/2}}$$

$$= -\frac{\mu_i}{r} \sum_{n=0}^{\infty} \left(\frac{r_i}{r}\right)^n P_n(\cos\psi_i) \tag{2}$$

where

$$\cos\psi_i = \frac{\mathbf{r}\cdot\mathbf{r}_i}{r r_i}$$

$$= \sin\theta\sin\theta_i + \cos\theta\cos\theta_i\cos(\lambda - \lambda_i) \tag{3}$$

Then, applying the addition theorem for Legendre poly-
nomials (Ref. 2, p. 328)

$$P_n(\cos\psi_i) = P_n(\sin\theta)P_n(\sin\theta_i) + 2\sum_{m=1}^{n}\frac{(n-m)!}{(n+m)!}P_n^m(\sin\theta)P_n^m(\sin\theta_i)\cos m(\lambda - \lambda_i) \tag{4}$$

12

Hence, if we write

$$C_{no}^i = \left(\frac{r_i}{R}\right)^n P_n (\sin \theta_i) \tag{5}$$

$$C_{nk}^i = 2\left(\frac{r_i}{R}\right)^n \frac{(n-k)!}{(n+k)!} P_n^k (\sin \theta_i) \cos k\lambda_i \tag{6}$$

$$S_{nk}^i = 2\left(\frac{r_i}{R}\right)^n \frac{(n-k)!}{(n+k)!} P_n^k (\sin \theta_i) \sin k\lambda_i \tag{7}$$

it follows that the potential ϕ_i may be written in standard form

$$\phi_i = -\frac{\mu_i}{r}\left[1 + \sum_{n=1}^{\infty}\sum_{m=0}^{n} \left(\frac{R}{r}\right)^n P_n^m (\sin \theta)(C_{nm}^i \cos m\lambda + S_{nm}^i \sin m\lambda) \right] \tag{8}$$

as an expansion about the center of the moon.

3. Example

An estimate of the Sjogren–Muller mascon distribution given in Table 4 has been expanded in spherical harmonics up to degree 15 according to the formulas of *Subsection 2*. A contour map based on the harmonic expansion and showing the corresponding bulges on a uniform-density moon are shown in Figs. 4 and 5. Table 5 identifies the level of each contour line by letter. It is interesting to note that this contour map, based on a fifteenth degree harmonic set, is quite adequate for identi-

fication of the mascon locations. A similar map using all the fourth degree harmonics plus zonals through degree eight completely failed to show the mascon locations.

References

1. Muller, P. M., and Sjogren, W. L., "Mascons: Lunar Mass Concentrations," *Science*, Vol. 161, No. 3842, pp. 680–684, Aug. 16, 1968.
2. Whittaker, E. T., and Watson, G. N., *A Course of Modern Analysis*, Fourth Edition. Cambridge University Press, 1927.

Table 4. Mascon locations and magnitudes

Number	Latitude, deg	Longitude, deg	Magnitude (fraction of lunar mass)
1	32	−17	0.23×10^{-4}
2	25	19	0.18×10^{-4}
3	18	56	0.10×10^{-4}
4	−15	33	0.09×10^{-4}
5	−23	−38	0.06×10^{-4}
6	−20	−95	0.12×10^{-4}
7	6	−6	0.07×10^{-4}
8	−6	−7	-0.10×10^{-4}
9	45	−35	-0.06×10^{-4}
10	11	15	-0.08×10^{-4}
11	−2	19	-0.08×10^{-4}

Table 5. Elevation contour key

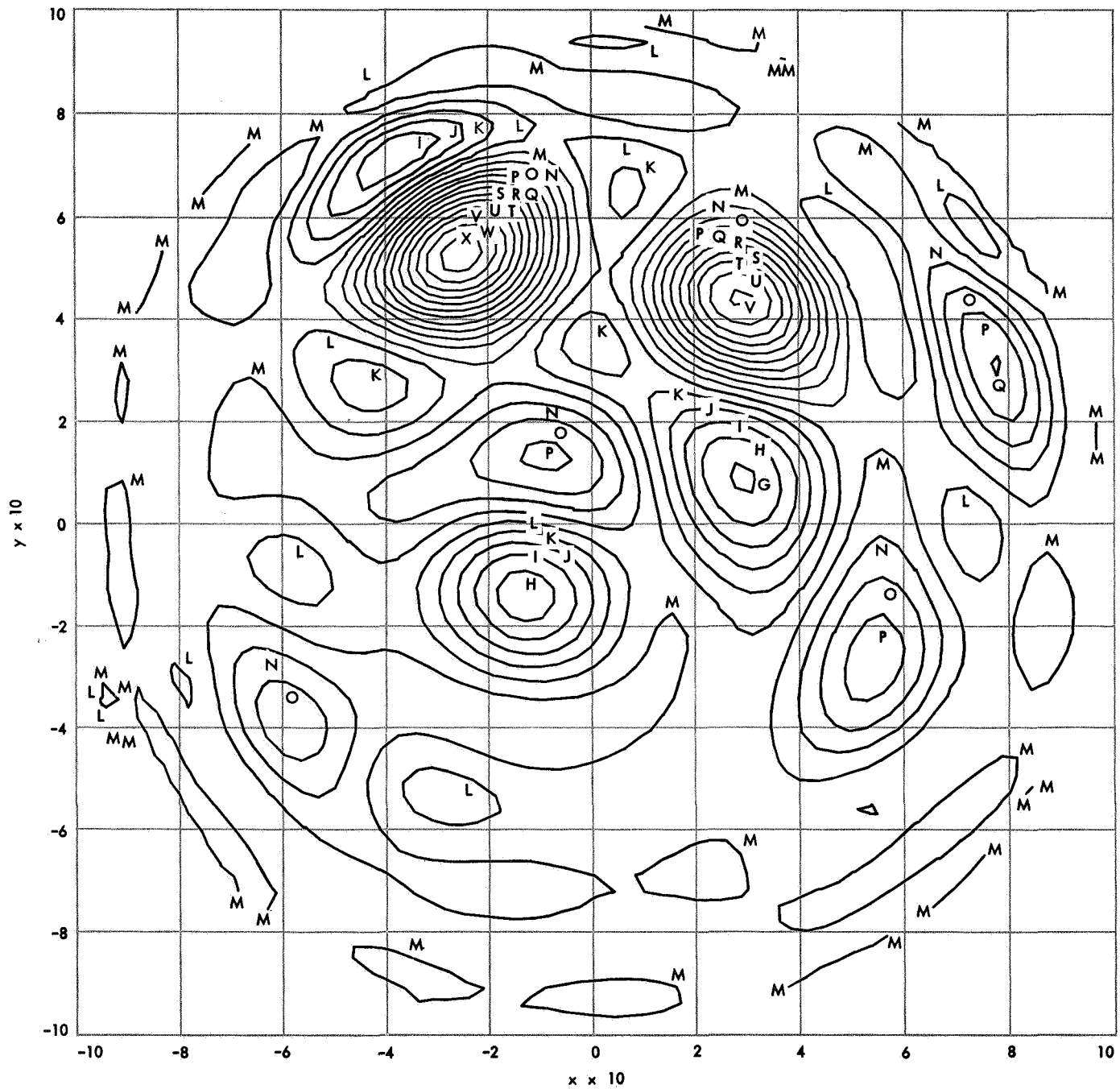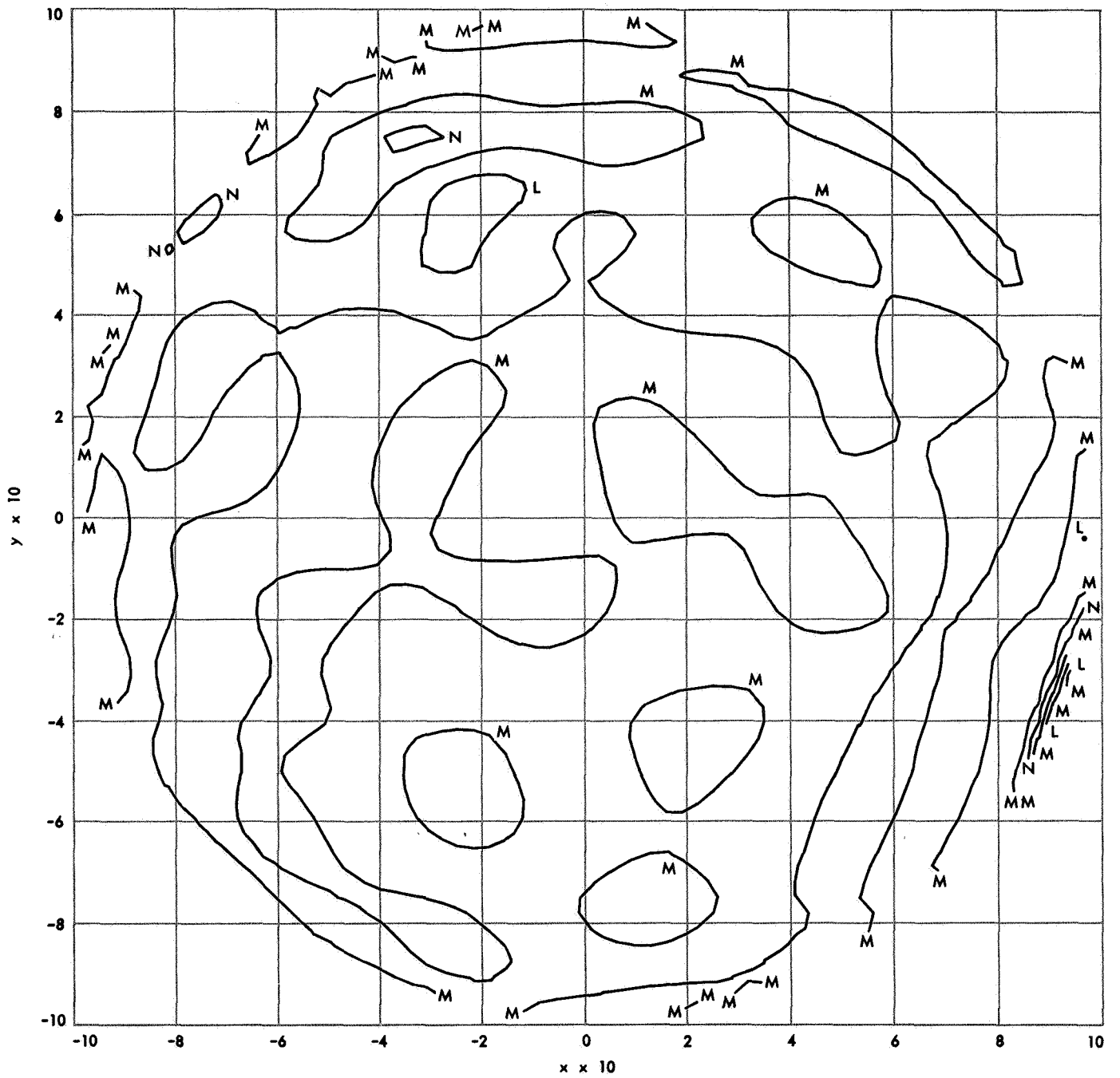| Arc	Contour value, m	Arc	Contour value, m
A	−3000	N	250
B	−2750	O	500
C	−2500	P	750
D	−2250	Q	1000
E	−2000	R	1250
F	−1750	S	1500
G	−1500	T	1750
H	−1250	U	2000
I	−1000	V	2250
J	−750	W	2500
K	−500	X	2750
L	−250	Y	3000
M	0		

Fig. 4. Mascon distribution on moon—front

Fig. 5. Mascon distribution on moon—back